Supporting Information for

Phosphate Buffer-Induced Depletion of Nickel Redox Sites Limits Oxygen Evolution on Stainless Steel Anodes

Kiho Nishioka[a*], Sakino Hiro[a], and Kuniaki Murase[a*]

[a]Department of Materials Science and Engineering, Kyoto University, Sakyo-ku, Kyoto 606-8501, Japan

**Address correspondence to:* nishioka.kiho.2h@kyoto-u.ac.jp, murase.kuniaki.2n@kyoto-u.ac.jp

Supporting Tables and Figures

Table S1 Physical properties of the electrolytes used in this study at 25 °C.

	Conductivity / S m^{-1}	Viscosity / mPa s
1 M KOH[1]	26.7	-
0.2 M K_2HPO_4 (pH11.5)	3.47	1.15
1 M K_2HPO_4 (pH11.5)	12.1	1.52
3 M K_2HPO_4 (pH11.5)	20.0	3.22

Table S2 Atomic fractions (at.%) determined by EDX analyses for a pristine bulk 304 SS sheet and a QCM-type 304 SS electrode.

	Bulk SS	QCM-type SS
Fe	65.73	64.26
Cr	16.68	16.37
Ni	8.59	7.31
Al	6.93	9.82
Mn	1.88	1.41

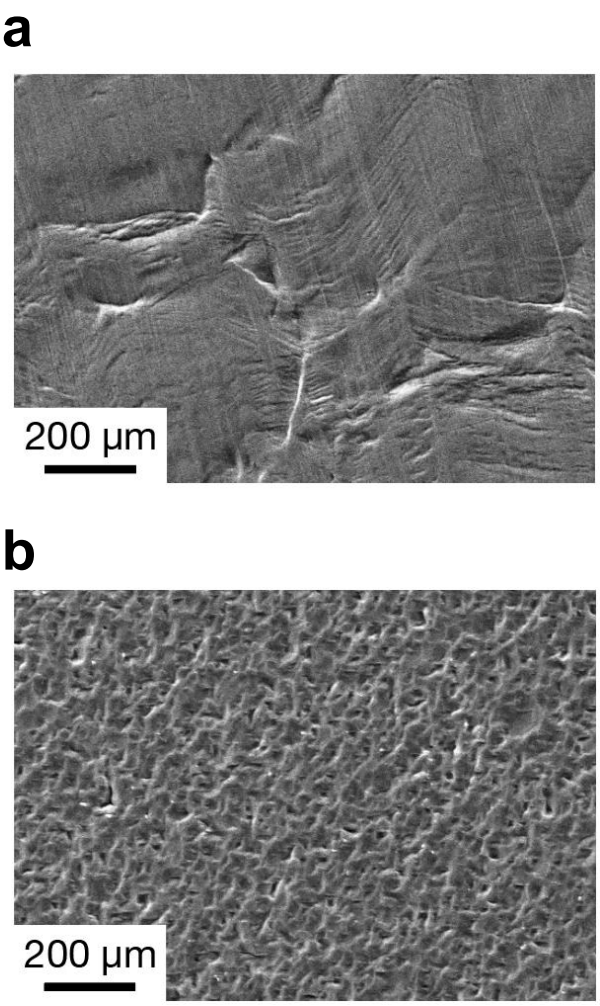

Figure S1. SEM images of pristine (a) bulk 304 SS sheet and (b) QCM-type 304 SS electrodes.

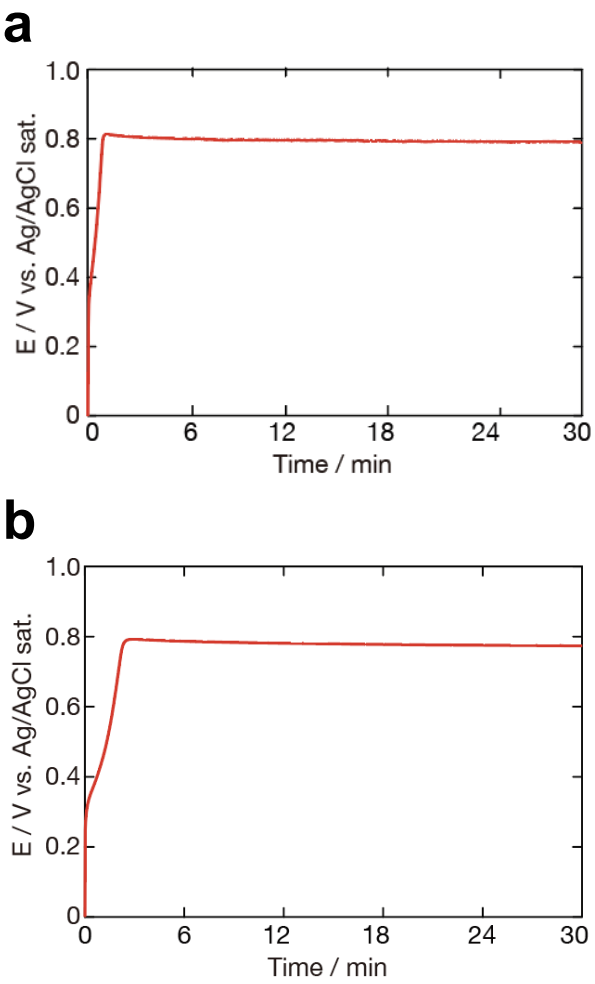

Figure S2. Time–potential curves recorded during galvanostatic electrolysis at 100 μA cm^{-2} using (a) bulk 304 SS and (b) QCM-type 304 SS electrodes in 1 M K_2HPO_4 (pH11.5).

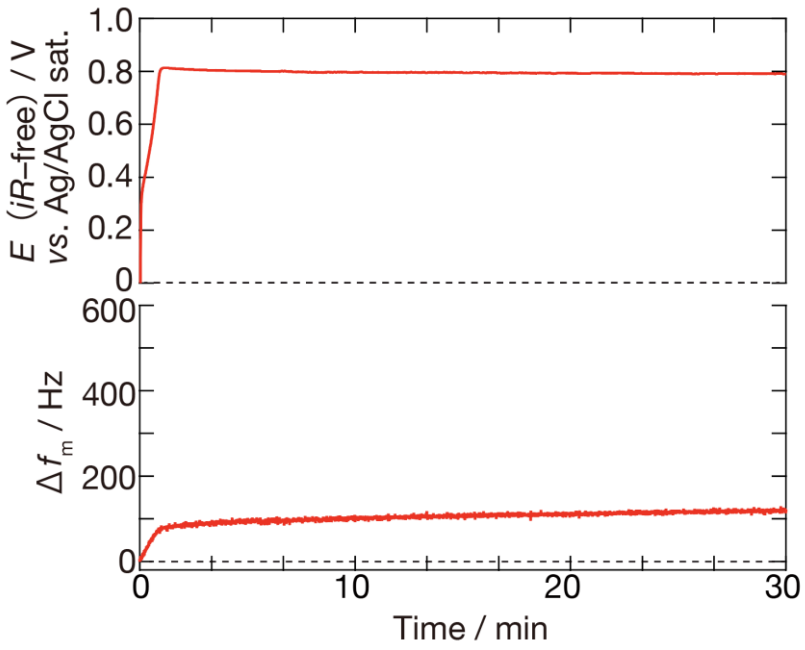

Figure S3. EQCM data obtained from a QCM-type 304 SS electrode at room temperature under a constant current of 100 μA cm^{-2} in 1 M K_2HPO_4 (pH11.5). The voltammogram and change in frequency are presented.

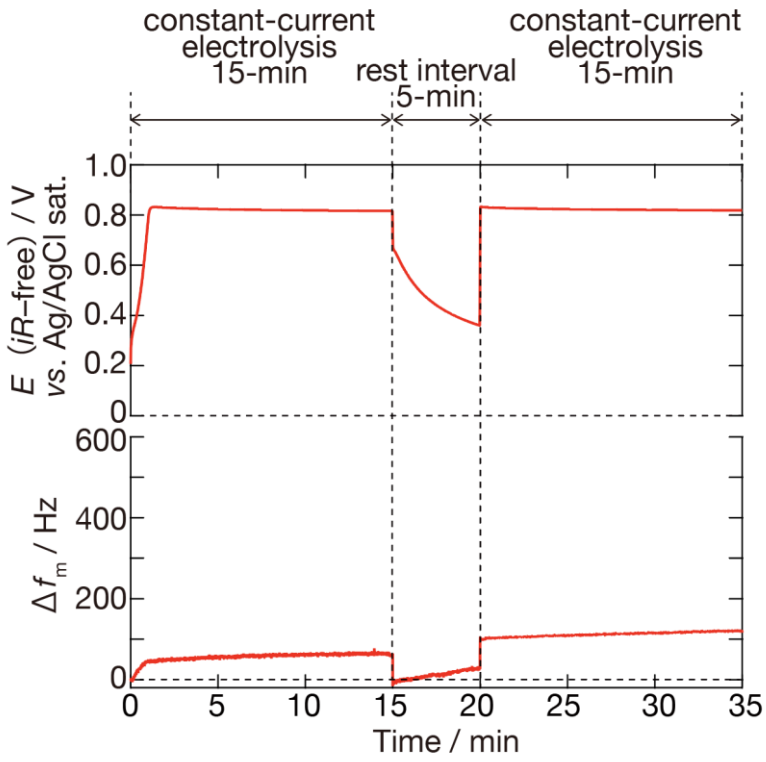

Figure S4. EQCM data obtained from the 304 SS electrode at room temperature during constant-current electrolysis at 10 μA cm^{-2} in 1 M K_2HPO_4 (pH 11.5). This trial included a 5 min rest interval between two electrolysis steps. The data indicate that the potential rapidly returned to 0.8 V upon restarting the electrolysis.

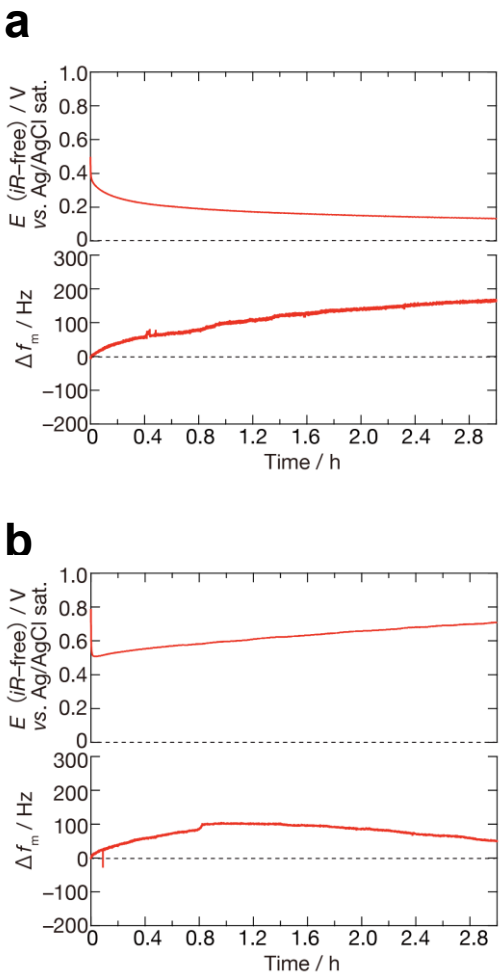

Figure S5. EQCM data obtained from a 304 SS electrode at room temperature under potentiostatic electrolysis conditions at (a) 0.4 and (b) 0.8 V in 1 M K_2HPO_4 (pH11.5), showing time-dependent changes in frequency.

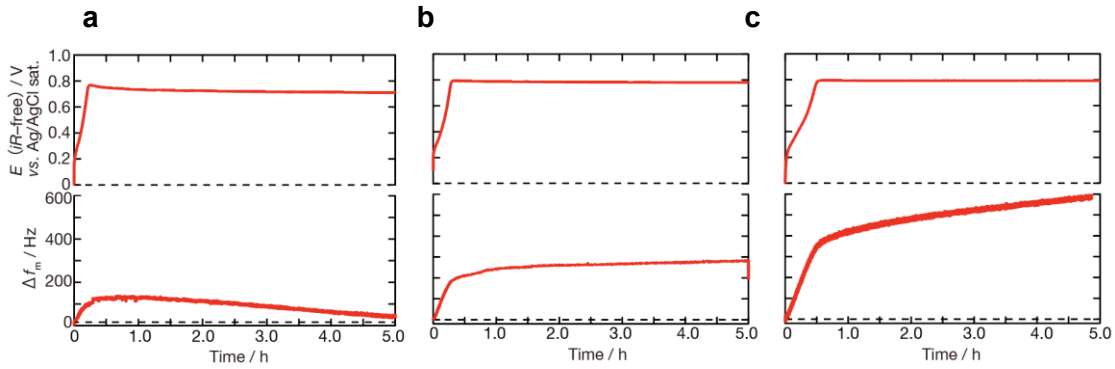

Figure S6. EQCM data acquired from a 304 SS electrode at room temperature under a constant current of 10 μA cm^{-2} in (a) 0.2, (b) 1, and (c) 3 M K_2HPO_4 solutions. All phosphate electrolytes used in this study were adjusted to pH 11.5.

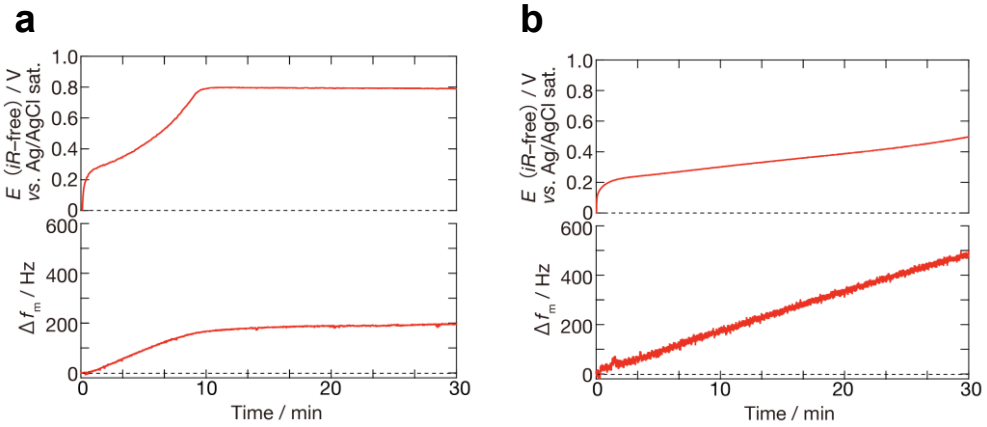

Figure S7. EQCM data obtained from a 304 SS electrode at room temperature under a constant current of 10 μA cm^{-2} over a duration of 30 min in (a) 1 and (b) 3 M K_2HPO_4 solutions. All phosphate electrolytes used in this study were adjusted to pH 11.5.

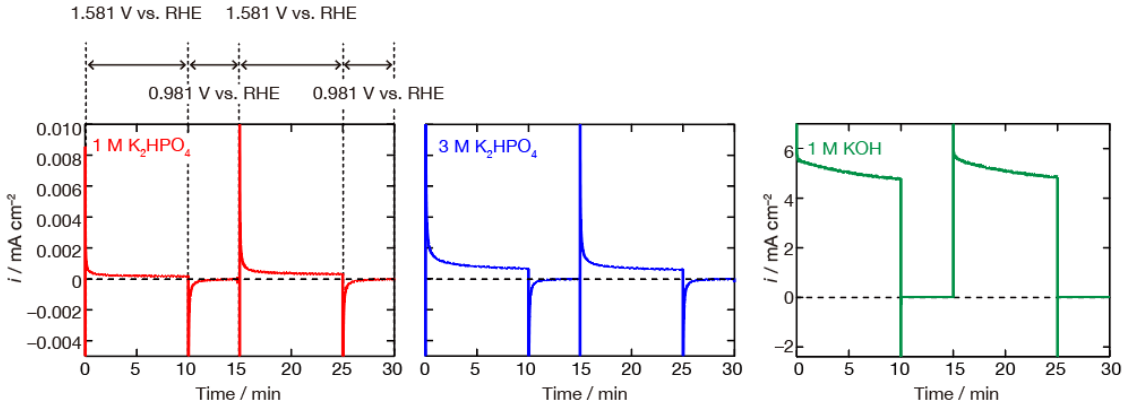

Figure S8. Current–time curves obtained from a 304 SS electrode during the twelfth cycle of potential steps between E = 1.581 V (10 min) and E = 0.981 V (5 min) in 1 M K_2HPO_4 (red), 3 M K_2HPO_4 (blue), and 1 M KOH (green) electrolytes. The details of this oxidation process are provided in the Experimental section.

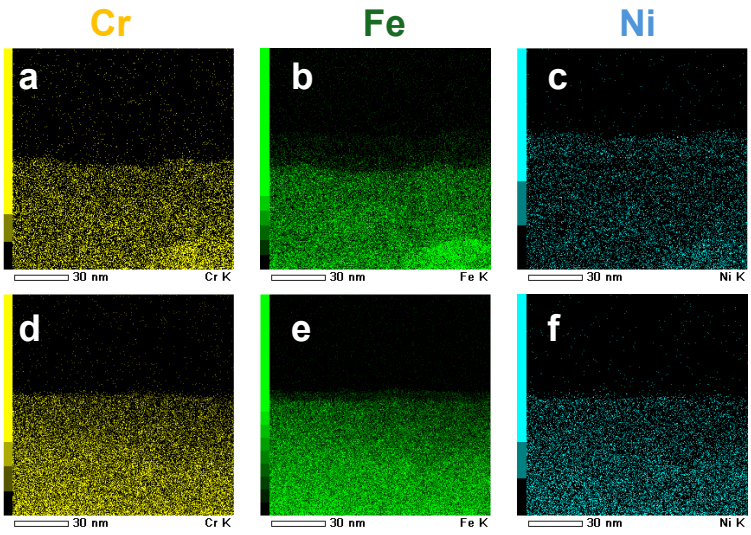

Figure S9. Cross-sectional EDX mapping images of a bulk 304 SS sheet electrode surface oxidized under previously reported conditions[2,3] in (a, b, c) 1 M KOH and (d, e, f) 1 M K_2HPO_4 solutions (pH 11.5). Panels (a, d), (b, e), and (c, f) show the distributions of Cr, Fe, and Ni, respectively.

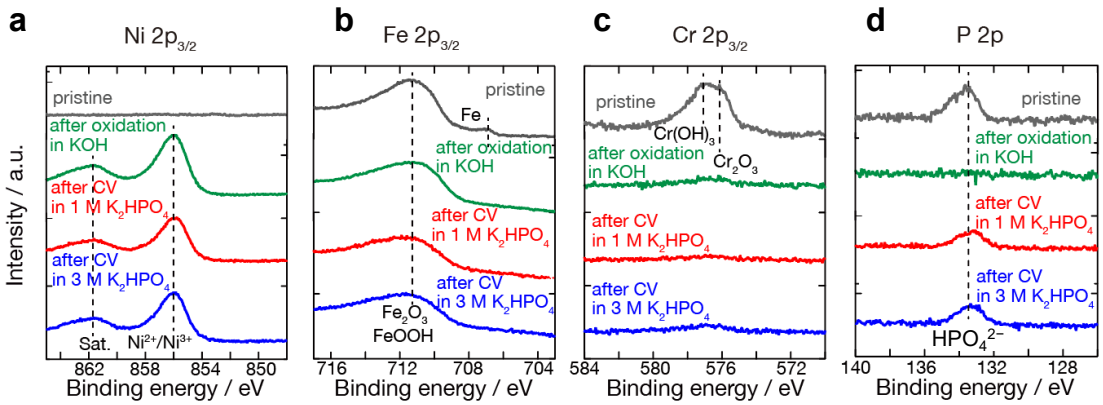

Figure S10 (a) Ni 2p, (b) Fe 2p, (c) Cr 2p, and (d) P 2p XPS data acquired from pristine 304 SS (gray), KOH-pretreated 304 SS (green), and KOH-pretreated 304 SS after CV in 1 M K_2HPO_4 (blue) and 3 M K_2HPO_4 (red) solutions.

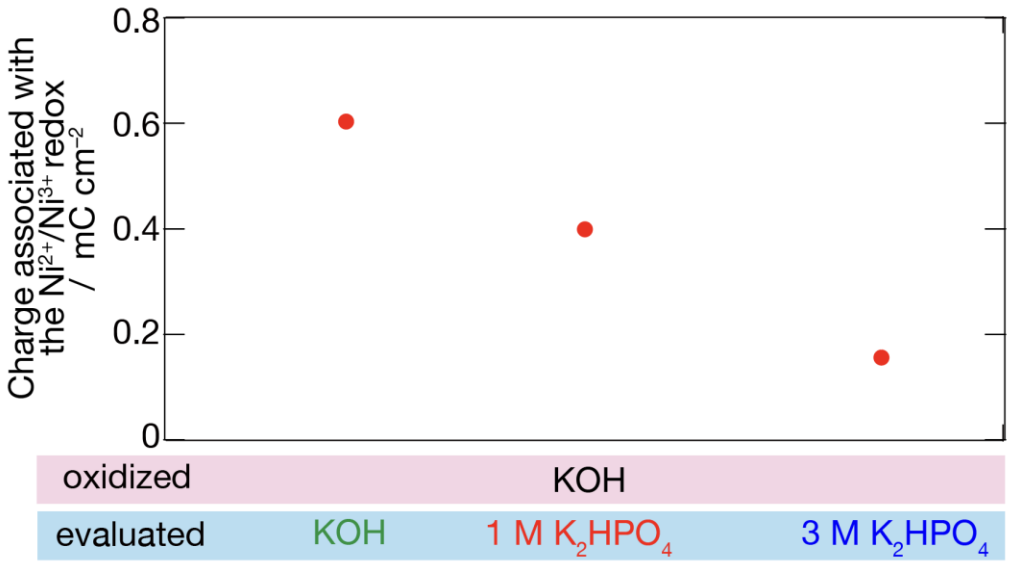

Figure S11 Charge capacity values for the Ni^{3+}/Ni^{2+} redox couple as determined from the cathodic peaks in CV data for the eleventh cycle. Electrodes were pretreated in 1 M KOH and subsequently evaluated in 1 M KOH, 1 M K_2HPO_4 or 3 M K_2HPO_4 solutions.

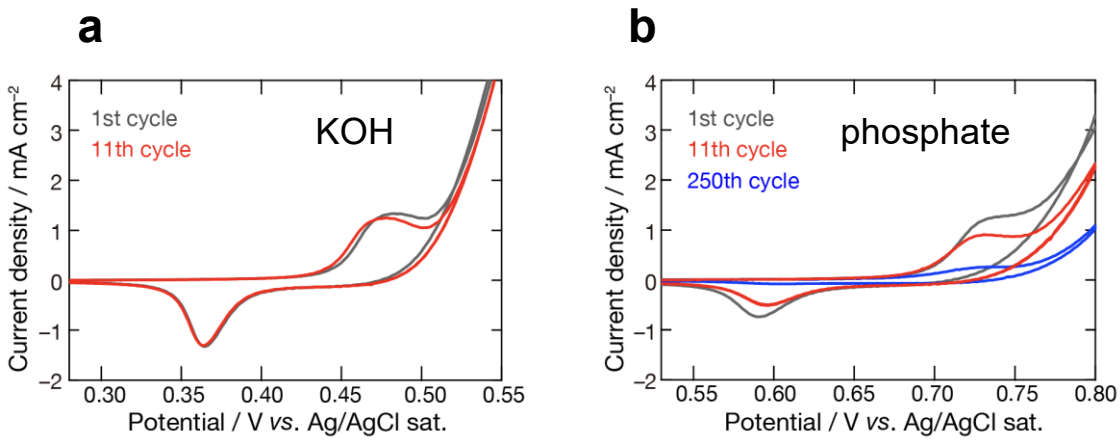

Figure S12. Cyclic voltammograms acquired at a scan rate of 50 mV s^{-1} to evaluate the Ni^{3+}/Ni^{2+} redox capacity of a 304 SS electrode in (a) KOH and (b) phosphate electrolytes.

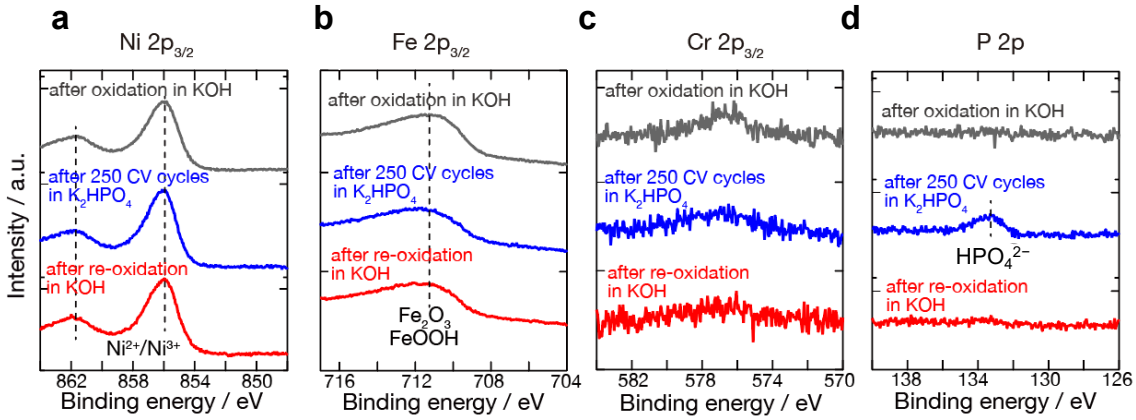

Figure S13. (a) Ni 2p, (b) Fe 2p, (c) Cr 2p and (d) P 2p XPS data obtained from a bulk 304 SS sheet electrode after KOH pretreatment (gray), subsequent 250 CV cycles in 1 M K_2HPO_4 electrolyte (blue), and subsequent re-oxidation in 1 M KOH (red). These CV trials were carried out at a scan rate of 50 mV s^{-1} at room temperature within the potential range of 0.5–0.8 V vs. Ag/AgCl sat. and correspond to Figures 6c–e in the main paper.

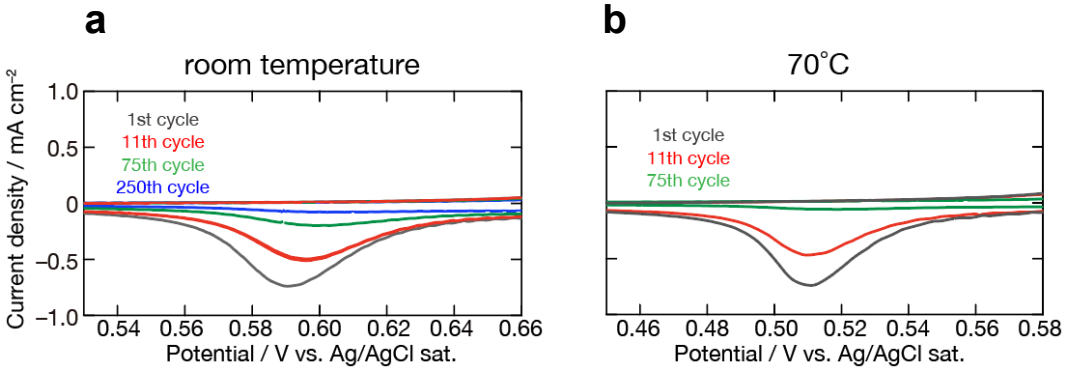

Figure S14. Cyclic voltammograms acquired at a scan rate of 50 mV s^{-1} to evaluate the Ni^{3+}/Ni^{2+} redox capacity of a 304 SS electrode in a phosphate electrolyte at (a) room temperature and (b) 70 °C.

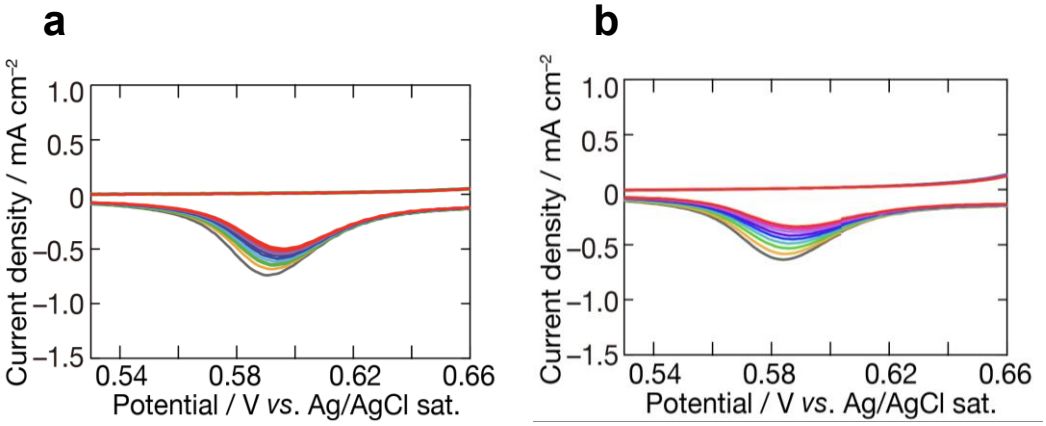

Figure S15. Cyclic voltammograms acquired at a scan rate of 50 mV s^{-1} to evaluate the Ni^{3+}/Ni^{2+} redox capacity of a 304 SS electrode in (a) 1 and (b) 3 M K_2HPO_4 solutions.

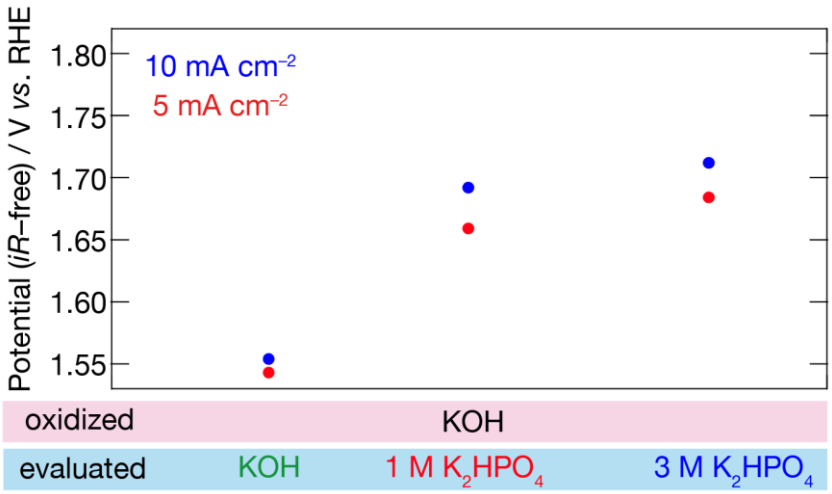

Figure S16. iR-free potentials of bulk 304 SS sheet electrodes at current densities of 5 and 10 mA cm^{-2} as determined from the cathodic peaks in the data obtained from the eleventh CV cycle. The electrodes were pretreated in 1 M KOH and subsequently evaluated for OER activity in 1 M KOH, 1 M K_2HPO_4 or 3 M K_2HPO_4.

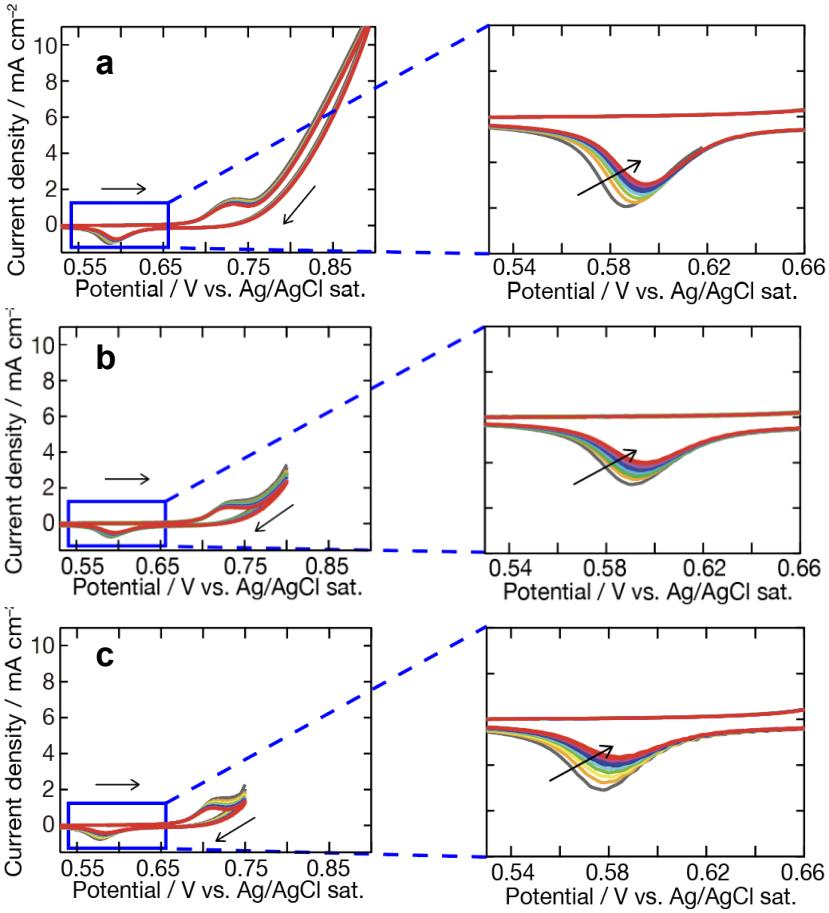

Figure S17. Cyclic voltammograms acquired at a scan rate of 50 mV s^{-1} to evaluate the Ni^{3+}/Ni^{2+} redox capacity of a 304 SS electrode in a phosphate electrolyte, using the potential regions (a) 0.4–0.9 V, (b) 0.4–0.8 V, and (c) 0.4–0.75 V vs. Ag/AgCl sat. The rightmost panels in each case show enlarged views of the Ni^{3+}/Ni^{2} redox region highlighted by blue boxes in the leftmost panels.

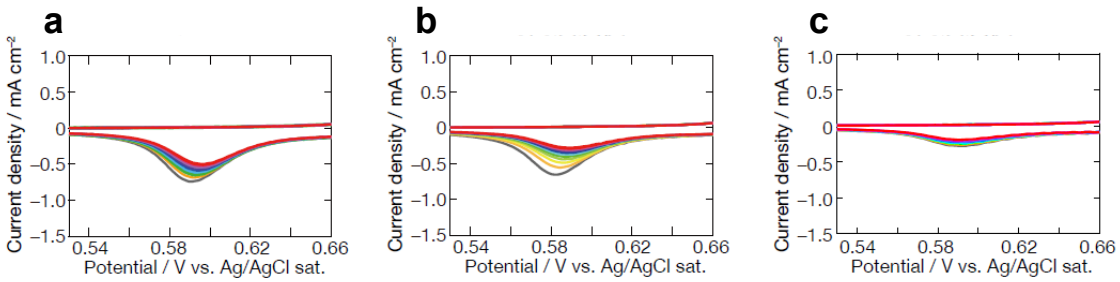

Figure S18. Cyclic voltammograms acquired at a scan rate of 50 mV s^{-1} to evaluate the Ni^{3+}/Ni^{2+} redox capacity of the 304 SS electrode in a phosphate electrolyte, generated following immersion in the electrolyte at the open-circuit potential for (a) 0 h (immediately after immersion), (b) 2 h, and (c) 8 h.

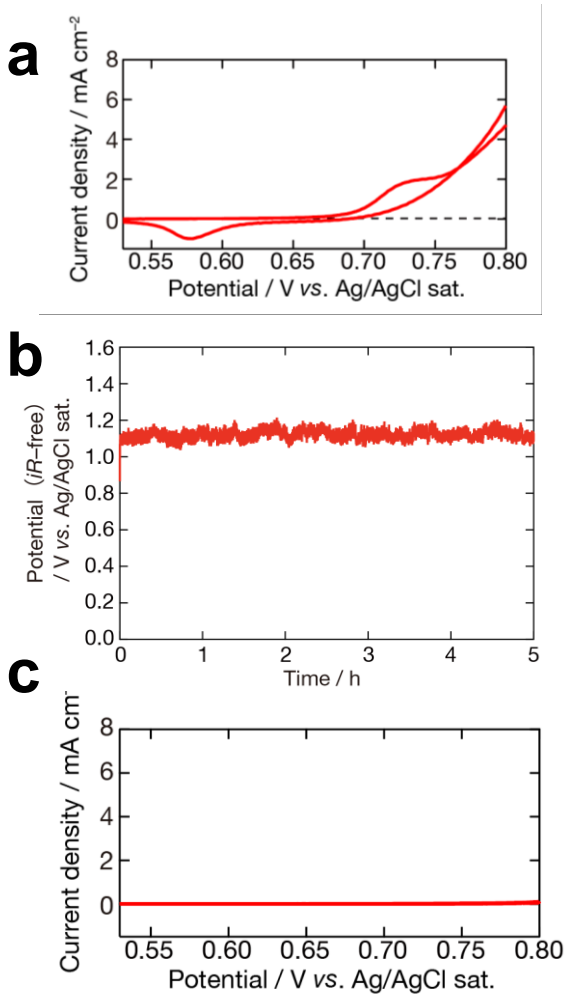

Figure S19. (a) Cyclic voltammogram recorded immediately after immersion in the electrolyte at a scan rate of 50 mV s^{-1}. (b) Potential–time curve recorded during galvanostatic electrolysis in 1 M K_2HPO_4 at 50 mA cm^{-2} over a duration of 5 h. (c) Cyclic voltammogram recorded at a scan rate of 50 mV s^{-1} following the galvanostatic electrolysis.

References

[1] R. GILLIAM, J. GRAYDON, D. KIRK, S. THORPE, *Int. J. Hydrogen Energy* **2007**, *32*, 359–364.

[2] F. Moureaux, P. Stevens, G. Toussaint, M. Chatenet, *Appl. Catal. B Environ.* **2019**, *258*, 117963.

[3] L. Magnier, G. Cossard, V. Martin, C. Pascal, V. Roche, E. Sibert, I. Shchedrina, R. Bousquet, V. Parry, M. Chatenet, *Nat. Mater.* **2024**, *23*, 252–261.